

**CURRENT STATUS OF THE RUN-BEYOND-CLADDING-  
BREACH (RBCB) TESTS**

**FOR THE INTEGRAL FAST REACTOR (IFR)**

**METALLIC FUELS PROGRAM  
DISCLAIMER**

This report was prepared as an account of work sponsored by an agency of the United States Government. Neither the United States Government nor any agency thereof, nor any of their employees, makes any warranty, express or implied, or assumes any legal liability or responsibility for the accuracy, completeness, or usefulness of any information, apparatus, product, or process disclosed, or represents that its use would not infringe privately owned rights. Reference herein to any specific commercial product, process, or service by trade name, trademark, manufacturer, or otherwise does not necessarily constitute or imply its endorsement, recommendation, or favoring by the United States Government or any agency thereof. The views and opinions of authors expressed herein do not necessarily state or reflect those of the United States Government or any agency thereof.

G. L. Batte'

G. L. Hofman

R. G. Pahl

Argonne National Laboratory

Argonne National Laboratory

P. O. Box 2528

9700 South Cass Avenue

Idaho Falls, ID 83403-2528

Argonne, IL 60439

MASTER

## LIST OF FIGURES

NUMBER		<u>PAGE</u>
1A	Element RT95 (MK-II, U-5Fs) XY-21A - Pre Run 139	2
1B	Metallographic of Exam Element RT95 Showing Crack	11
2	Longitudinal Section From the Dimple Region of Element Macrograph Shows Restructured Material at the End of the Fuel Pin	12
3	XY-24: Fuel Clad Interaction and Restructuring Comparisons	14
4	XY-27 Element J432 Breach	16
5	Typical Release Sequence	17
6	X482 DN Signal During Breach	20
7	X482 Metallographic Exams	21
8	Transverse Section Through the Fuel Column Breach Site. The Arrow Indicates Location of the Crack Which is not Visible at this Magnification	24
9	Figure 9 Compares the DN Signals from the Artificially Induced Breach of the IFR RCB Experiment X482 with That of the Naturally Occurring Breach in the Lead IFR Subassembly X420. Note the Similarities in the Initial Short Duration "Spikes" Followed by the Signal Return to Background.	26

## LIST OF TABLES

I	RBCB Program Status	5
II	Analytical Results of IFR RBCB Experiments	10

## ABSTRACT

This paper describes the results from the Integral Fast Reactor (IFR) metallic fuel Run-Beyond-Cladding-Breach (RBCB) experiments conducted in the Experimental Breeder Reactor II (EBR-II). Included in the report are scoping test results and the data collected from the prototypical tests as well as the exam results and discussion from a naturally occurring breach of one of the lead IFR fuel tests. All results showed a characteristic delayed neutron and fission gas release pattern that readily allows for identification and evaluation of cladding breach events. Also, cladding breaches are very small and do not propagate during extensive post breach operation. Loss of fuel from breached cladding was found to be insignificant. The paper will conclude with a brief description of future RBCB experiments planned for irradiation in EBR-II.

## INTRODUCTION

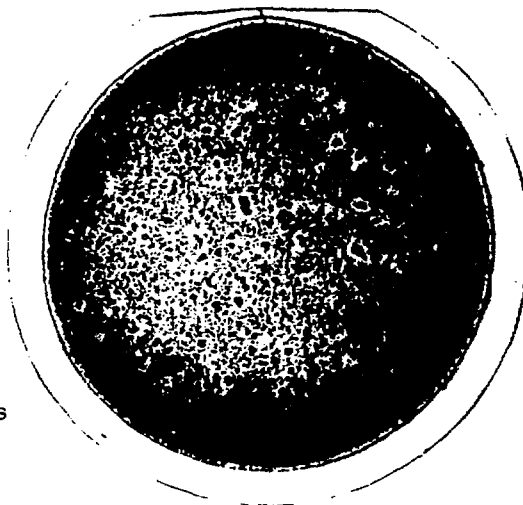
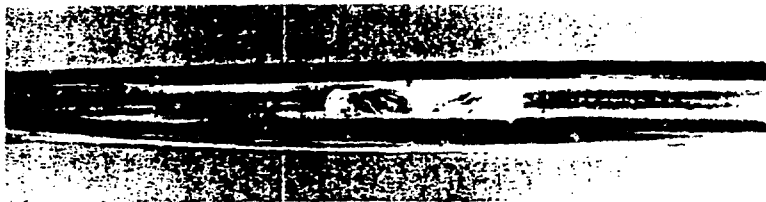
In 1985, Argonne National Laboratory (ANL) began the development of an advanced-design metallic fuel based on uranium zirconium (U-Zr) and uranium-plutonium-zirconium (U-Pu-Zr) alloys. During the past five years several areas were addressed concerning the performance of this fuel system. Metallic fuel has demonstrated its ability to perform reliably to high burnups under varying operating conditions. This paper will present one area of testing which concerns the fuel system's performance under cladding breach conditions.

Each Run-Beyond-Cladding-Breach (RBCB) experiment consisted of a single element test in which cladding breach was artificially-induced. This was accomplished by machining a thin area in the cladding of a preirradiated test element and allowing it to breach during further irradiation (Fig. 1A). Several tests were conducted using different ternary fuel alloys of U-xPu-10Zr (x = 0-19 wt %) clad with D9, HT9, and Type-316 stainless steel cladding materials. The initial scoping tests were designed around EBR-II MK-II driver fuel using 4.4 mm (0.174 in.) diameter fuel pins clad in solution-annealed 316 SS with the wire wrap removed. The subsequent testing used fuel pins 5.8 mm (0.230 in.) in diameter, more typical of IFR designs. The test pins were previously irradiated to a range of heavy metal burnups between 3 and 12 at.%. Steady-state irradiation and subsequent Post-Irradiation- Examination (PIE) of the RBCB tests have resulted in a large data

Fig. 1A. Element RT95 (MK-II, U-5Fs) XY-21A - Pre Run 139

ELEMENT RT95 (MK-II, U-5Fs)  
XY21A

PRE RUN 139



TRANSVERSE VIEW OF CRACK IN RT95  
DEFECT. THINNED CLAD MEASURES 2.5 MILS  
IN THICKNESS AT THIS POINT. ELEVATION  
SHOWN IS APPROXIMATELY 50 MILS FROM  
THE ORIGINAL SAW CUT AND 7 MILS FROM  
FIRST BREACH INDICATION

base that has produced strong support of the fuel's expected benign behavior under breach conditions. Table I provides a description of the IFR RBCB program and its current status.

## PHASE 1

### IRRADIATION DATA

Experiment XY-21 was the first in a series of scoping tests to evaluate the failure behavior of metal fuel for the IFR program. The experiment used irradiated U-5Fs\* fuel because irradiated ternary fuel was not yet available. It was positioned under the BFTR (Breached Fuel Test Facility) and was scheduled to be irradiated for one reactor run. The 61-pin fuel bundle consisted of 60 fresh Mark-II core driver fuel elements and one high burnup (7-8 at.%) Mark-II (U-5Fs) test element. The test element had flat (using a 7/16 in. end mill), prethinned machined area placed at 25.4 cm (10 in.) from the bottom of the element leaving a clad wall of 100  $\mu\text{m}$  (4 mils). The test element was xenon tagged and was expected to breach during or shortly after reactor startup according to stress-rupture calculations. However, the test element did not fail. Experiment XY-21 operated for ~40 days (2182 MWd) during reactor run 136 without cladding breach. Test element NN-41 achieved a peak burnup of 7.91 at.%, equal to the administrative bu limit of 8 at.%. At the end of the run, XY-21 was removed from the reactor for postirradiation examination (PIE).

\*Fission (Fs) is an equilibrium concentration of fission-product elements that remain after the pyrometallurgical reprocessing cycle originally designed for EBR-II. It consists of 2.4 w.% molybdenum, 1.9w.% ruthenium, 0.3 wt.% rhodium, 0.2 wt.% palladium, 0.1 wt.% zirconium, and 0.1 wt.% niobium, with 0.05 wt.% Si added for improved irradiation performance.

XY-21A, essentially a reconstitution of XY-21, consisted of a fuel bundle using the original 60 filler elements from XY-21 and a new high burnup test element. Since the test element in XY-21 failed to breach, the XY-21A test element had a machined area that left the clad wall at a thickness of only 38  $\mu\text{m}$  (2.5 mils) versus 100  $\mu\text{m}$  (4 mil) wall of XY-21. The test element was not xenon tagged.

Experiment XY-21A was irradiated under the FPTF (Fission Product Test Facility) for ~60 days (3348 MWd) during reactor run 139. Both the BFTF and FPTF facilities allow for enhanced fission product detection by incorporating DN detection instrumentation specific to their respective facilities. XY-21A did undergo a breach after six days. Breach detection was indicated by a slight increase in delayed neutron (DN) counts on the FPTF DN detector (~30-40 cps for about 3 hours) as well as a corresponding indication of increased gas activity on the Germanium-Lithium-Argon-Sampling-System (GLASS). XY-21A was removed from the reactor and the test element (RT-95) achieved a peak burnup of 9.3 at.%. Of the sixty days, ~54 were under a breached condition.

Experiment XY-24 was an RBCB experiment designed to evaluate the failure behavior of IFR ternary-alloy fuel. It consisted of a subassembly containing 59 standard Mark-II elements (U-5Fs) and two Mark-II size U-19Pu-10Zr elements that had a machined thinning of the wall 25.4 cm (~10 in.) from the bottom of the fuel column leaving a clad wall 25-50 mm (~1-2 mils) thick. The two test elements were fabricated with a double sodium bond load (reduced

RBCB Program Status  
TABLE 1

Category/Info	Scoping Tests Phase I			IFR Prototypic Phase II			Natural Breaches
	XY-21/21A	XY-24	XY-27	X482	X482A	X482B	
Experiment ID#	XY-21/21A	XY-24	XY-27	X482	X482A	X482B	X420B
Composition, wt%	U-5Fs	U-19Pu-10Zr	U-8Pu-10Zr	U-19Pu-10Zr	U-10Zr	U-19Pu-10Zr	U-19Pu-10Zr
Cladding Material	316SS	316SS	316SS	D9	D9	HT9	D9
Final Burnup, at.%	~9.3	~7.5	~6.0	14.4	13.5	~14.0	~17.0
Element Diam., mm	4.4	4.4	4.4	5.8	5.8	5.8	5.8
#of Days Breached	54	233	131	168	~100	~190	34
RUNS	136-139	143-146	144-146	149-150	152-153	154-155	150B
STATUS OF TEST ELEMENT	NN41(XY-21) no breach RT95(XY-21A) breached	J507 breached J516 no breach	J432 breached J486 breached	T139 breached	T045 breached	T464 breached on startup of Run 154 ,ID'd by xenon tag	Natural breach in fuel column at 10" elevation Element T084
DN Signal, cps (1)	~30-40	note (2)	note (2)	~600	~700	note (3)	~1000
Weight Loss, g (4)	~2.0	2.7	~2.5	4.04	3.61	not available(5)	4.1
Core Location	BTF	FPTF	BTF	Open Core	Open Core	Open Core	Open Core

**Notes:**  
 (1) counts above background  
 (2) unavailable due to malfunction of instrument sensitivity  
 (3) none detected, possibly breached in basket  
 (4) expulsion of bond sodium+fission gas+cesium accounts for majority of weight loss; there was negligible fuel loss  
 (5) will be removed from reactor late 1990

plenum volume) to simulate a higher burnup pressure in the plenum. XY-24 was irradiated under the FPTF for 320 days during reactor runs 143 through 146. The test elements were not xenon tagged. The test elements (J507 and J516) had been previously irradiated in subassembly X428 during runs 140 and 141 to a burnup of ~3 at.%. Breach was detected ~74 days after insertion giving XY-24 223 days irradiation after breach. XY-24 was removed from the reactor at the end of run 146 for PIE. Elements J507 and J516 had both achieved a peak burnup of 7.6 at.%, respectively. Indications from XY-24 and YX-27 (see below) were similar in that very little DN signal was observed and the major indication of failure was in fission gas activity.

Experiment XY-27 was an RBCB experiment similar to XY-24, designed to evaluate the failure behavior of a second IFR ternary-alloy fuel with lower Pu content. It consisted of a subassembly containing 59 standard Mark-II elements (U-5Fs) and two Mark-II size U-8Pu-10Zr elements that had a machined thinning of the wall 25.4 cm (~10 in.) from the bottom of the fuel column leaving a clad wall 25-50  $\mu\text{m}$  (~1-2 mils) thick. The two test elements were also fabricated with a double sodium bond load to simulate a plenum pressure typical of higher burnup. XY-27 was located under the Breached-Fuel-Test-Facility (BFTF) and was irradiated for three reactor runs (Runs 144-146). The test elements were not xenon tagged. The test elements (J486 and J432) had been previously irradiated in subassembly X428 during runs 140 and 141 to a burnup of ~3 at.%. Breach was detected ~123 days after insertion giving

XY-27 131 days irradiation after breach. XY-27 was removed from the reactor at the end of run 146 for PIE. Elements J486 and J432 had achieved a peak burnup of 6.6 and 6.7 at.%, respectively.

## POSTIRRADIATION ANALYSIS

Both nondestructive and destructive examinations were conducted on the IFR RBCB scoping test elements. Nondestructive examinations included: visual examination and photographic documentation of the test elements and subassembly element bundles; test element weighing; gamma scanning; profilometry; analytical analysis of suspect smears and neutron radiography. Destructive examination consisted of sectioning the test elements at various elevations, both axially and radially, for metallographic examination. The metallographic examinations were concentrated on two areas in the test elements:

1. The area around the machined defect to study the cladding failure condition and the structure of the fuel immediately adjacent to the crack.
2. The top of the fuel slug region to study the degree of fuel restructuring due to an increase of fuel temperature after loss bond sodium through the breach. Because sodium logging in the fuel effectively raises the thermal conductivity, some fuel overheating was expected.

Element NN-41 (Subassembly XY-21) with its clad wall thinned to 25% of its original thickness and at a burnup of  $\approx 8$  at.% sustained a

period of 36 days irradiation without incurring a breach. Evidently the calculation of time to rupture using plenum gas pressure and existing creep rupture properties was not appropriate for these conditions (fuel column breach, defected cladding). Visual inspection revealed no apparent breach and no difference between pre- and postirradiation weights was measured. Although no breach had occurred, metallography revealed that small cracks had formed in the thinned area and that the 100  $\mu\text{m}$  (4 mil) thinned area of the wall was distorted by creep. A transverse section through the thinned region showed a bulge measuring about 32  $\mu\text{m}$  (1.25 mils). There exists a dense outer zone at the fuel slug perimeter which has previously been shown to be Ni rich and harder than the rest of the fuel. It is possible that this zone distributes the pressure load on the thinned cladding area, thereby making the time-to-rupture calculation for the thinned area based on biaxial gas loading invalid. No further analyses were performed on NN-41.

With element RT-95 (subassembly XY-21A), the potential of a breach was enhanced by thinning the clad wall to 38  $\mu\text{m}$  (2.5 mils), ~18% of its original thickness. Upon disassembly, evidence of a clad breach was observed by the accumulation of sodium test. Prior to removing the sodium globule, the element was weighed revealing that the element weight had decreased by 2.07 grams. The sodium globule was removed from the face of the thinned area for chemical analysis. Essentially no fuel was lost through the breach as chemical analysis revealed negligible amounts of fuel (Table II) in the sample. The 2 gram weight can be attributed to the amount of sodium bond and fission gas expulsion. Gamma scans indicated that the sodium bond

and associated fission products, including Cs, were indeed lost through the breach. A transverse metallographic sample taken through the breach revealed a crack through the 38  $\mu\text{m}$  (2.5 mil) thinned wall 750  $\mu\text{m}$  (30 mils) in length (Fig. 1B). Metallographic examination of the top of the fuel slug revealed that some restructuring had occurred due to the loss of the bond sodium (Fig. 2). Results of plenum analysis showed a gas volume of 1.85 cc and a pressure of 125 psia indicating that the majority of the plenum gas had been expelled from the element.

Of the two test elements from XY-24, element J-516 showed no visual evidence of breach. J-516 had achieved a peak burnup of 7.6 at.%. The cladding wall had been thinned from 300 to 75  $\mu\text{m}$  (12 to ~3 mils) and the lack of breach to this burnup was unexpected, perhaps showing that fuel/clad bonding may have reduced the cladding stress. Further indication of element integrity was supported by weighing which revealed no change in the pre- and postirradiated element weights. The gamma scan data indicated the existence of bond sodium, containing Cs, in the plenum. Metallurgical samples of the thinned area and top of fuel column revealed that the clad wall was intact and that the top of the fuel column had not undergone restructuring. Plenum gas analysis showed a plenum volume of 0.23 cc with a pressure of 2066 psia at room temperature, indicating that the plenum inventory was still intact.

TABLE II  
Analytical Results of IFR RBCB Experiments

S/A#	ELEMENT	SMEAR NUMBER	S/A#	ELEMENT	WEIGHT LOSS(G)	BURNUP (A/O)	Composition (Wt%)	Uranium $\mu\text{g/sm}$ or $\text{samp}$	Plutonium $\mu\text{g/sm}$ or $\text{samp}$	Nb-95	Zr-95	Ru-106	Cs-134
X-482	T-139	#69( $\mu\text{Ci/smear}$ )	X-482	T-139	4.04	12.2	U-19Pu-10Zr		0.6				2
X-482	T-139	Samp.Vial( $\mu\text{Ci/samp}$ )	X-482	T-139	4.04	12.2	U-19Pu-10Zr		64				1700
XY-21A	RT-95	#J-382( $\mu\text{Ci/smear}$ )	XY-21A	RT-95	2.07	9.3	U-5Fs			0.765	0.437	1.08	0.062
XY-21A	RT-95	#J-331( $\mu\text{Ci/smear}$ )	XY-21A	RT-95	2.07	9.3	U-5Fs			n.d.	3.06	n.d.	0.139
XY-21A	RT-95	#J-386( $\mu\text{Ci/smear}$ )	XY-21A	RT-95	2.07	9.3	U-5Fs			0.137	n.d.	n.d.	0.061
XY-21A	RT-95	#J-327( $\mu\text{Ci/smear}$ )	XY-21A	RT-95	2.07	9.3	U-5Fs			0.176	0.178	n.d.	n.d.
XY-21A	RT-95	*Blob( $\mu\text{Ci/samp}$ )	XY-21A	RT-95	2.07	9.3	U-5Fs	350	0.2				
XY-24	J-516	#M-445( $\mu\text{Ci/smear}$ )	XY-24	J-516	0.00	7.5	U-19Pu-10Zr	<3.0	0.007				n.d.
XY-24	J-507	#M-401( $\mu\text{Ci/smear}$ )	XY-24	J-507	2.73	7.5	U-19Pu-10Zr	<3.0	0.95				42
XY-24	J-507	Can#S2( $\mu\text{Ci/samp}$ )	XY-24	J-507	2.73	7.5	U-19Pu-10Zr	<150	6.2		390		
XY-27	J-432	#M-408( $\mu\text{Ci/smear}$ )	XY-27	J-432	2.45	6	U-8Pu-10Zr	7	0.15				40
XY-27	J-432	#M-44( $\mu\text{Ci/smear}$ )	XY-27	J-432	2.45	6	U-8Pu-10Zr	<300	7.3				60
XY-27	J-486	#M-405( $\mu\text{Ci/smear}$ )	XY-27	J-486	2.60	6	U-8Pu-10Zr	<3	0.15				24
XY-27	J-486	#M-43( $\mu\text{Ci/smear}$ )	XY-27	J-486	2.60	6	U-8Pu-10Zr	<3	1.6				400
S/A#	ELEMENT	SMEAR NUMBER	S/A#	ELEMENT	Cs-137	Ba-140	La-140	Ce-141	Ce-144	Eu-154	Eu-155	Others	
X-482	T-139	#69( $\mu\text{Ci/smear}$ )	X-482	T-139	19	3.2	3.8		4.4	0.2	1.9		
X-482	T-139	Samp.Vial( $\mu\text{Ci/samp}$ )	X-482	T-139	16000	3600	4600		1800	600	5100		
XY-21A	RT-95	#J-382( $\mu\text{Ci/smear}$ )	XY-21A	RT-95	0.865	n.d.	0.114	n.d.	4.27	n.d.	0.103		
XY-21A	RT-95	#J-331( $\mu\text{Ci/smear}$ )	XY-21A	RT-95	3.75	34.8	41	0.46	2.52	6.6	25.2		
XY-21A	RT-95	#J-386( $\mu\text{Ci/smear}$ )	XY-21A	RT-95	1.14	1.38	1.45	n.d.	0.466	0.277	1.09		
XY-21A	RT-95	#J-327( $\mu\text{Ci/smear}$ )	XY-21A	RT-95	0.31	0.5	0.7	n.d.	0.92	0.093	0.341		
XY-21A	RT-95	*Blob( $\mu\text{Ci/samp}$ )	XY-21A	RT-95	2	188	239			10	28		
XY-24	J-516	#M-445( $\mu\text{Ci/smear}$ )	XY-24	J-516	0.2	0.6	0.7			n.d.	0.3	.2(Mn-54)	.9(Co-58)
XY-24	J-507	#M-401( $\mu\text{Ci/smear}$ )	XY-24	J-507	700	1100	1400			360	4000		40(Co-58)
XY-24	J-507	Can#S2( $\mu\text{Ci/samp}$ )	XY-24	J-507	520	2600	3700			5100	48000	2100(Na-22)	
XY-27	J-432	#M-408( $\mu\text{Ci/smear}$ )	XY-27	J-432	540	290	390			n.d.	120		
XY-27	J-432	#M-44( $\mu\text{Ci/smear}$ )	XY-27	J-432	800	630	830			25	330		
XY-27	J-486	#M-405( $\mu\text{Ci/smear}$ )	XY-27	J-486	310	520	700			14	190		
XY-27	J-486	#M-43( $\mu\text{Ci/smear}$ )	XY-27	J-486	4100	19000	26000			n.d.	5300		

Fig. 1B. Metallographic of Exam Element RT95 Showing Crack

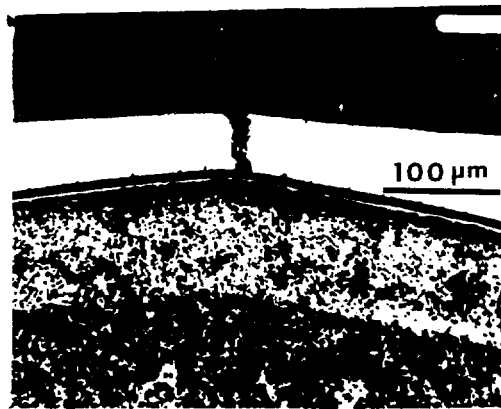


Fig. 2. Longitudinal Section From the Dimple Region of Element  
Macrograph Shows Restructured Material at the End of the  
Fuel Pin.

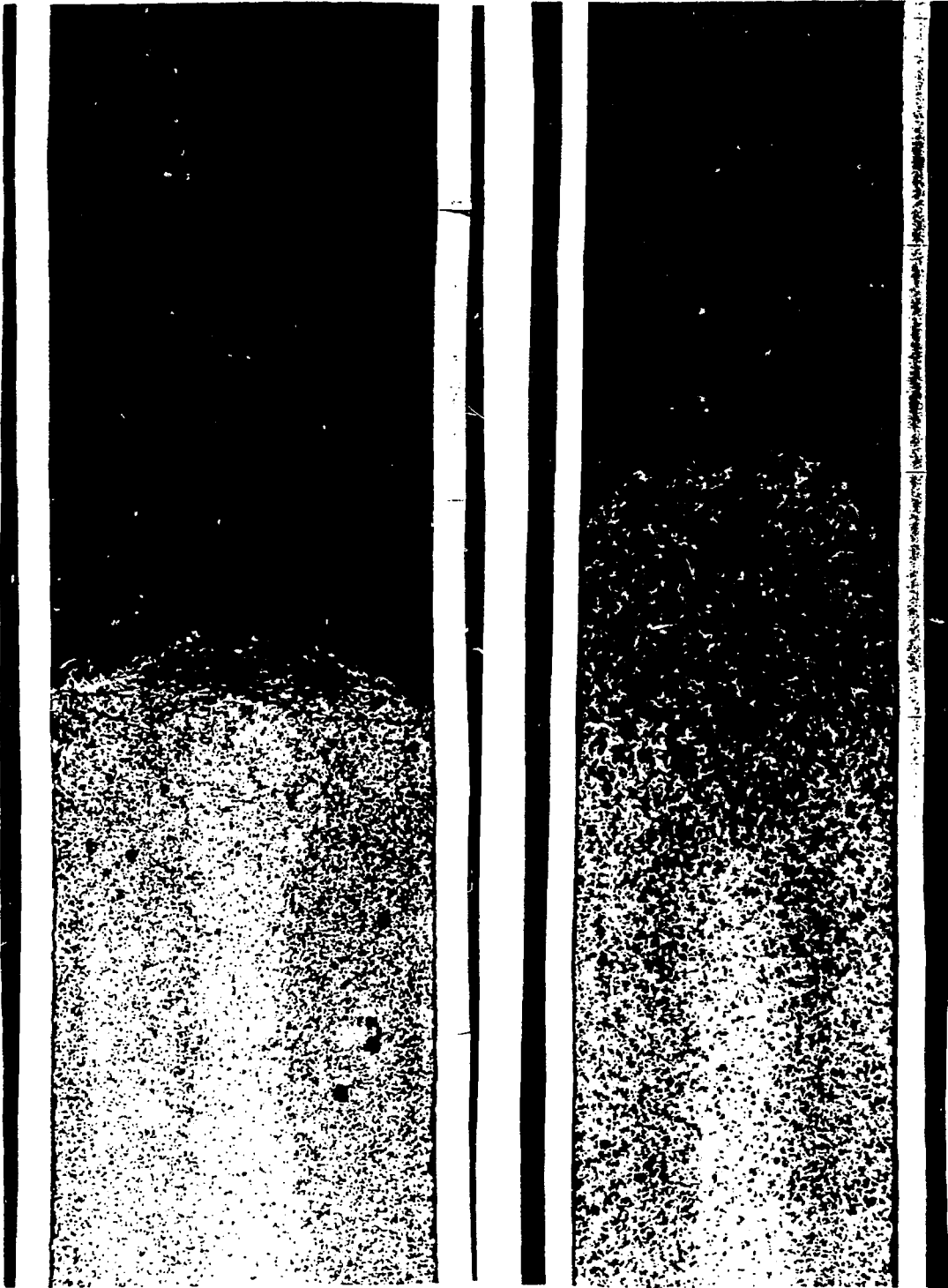


The second test element, J-507 (XY-24), did show signs of breach upon visual inspection in the form of traces of sodium at the thinned area. When weighed, the element showed a loss of 2.73 grams which could be accounted for by the loss of sodium bond (2 g) and fission gases. Element J-507 achieved a peak burnup of 7.6 at.%. Plenum gas analysis showed a plenum volume of 2.39 cc with a pressure of 26 psia at room temperature. As in the case of RT-95, gamma scans revealed loss of sodium bond. Metallographic exams reveals a small pin-hole type crack had occurred on the face of the thinned area and that the top of the fuel slug had undergone some restructuring due to the loss of the bond sodium.

Figure 3 shows the difference between element J516 (no breach) and element J507 (breach) in the area of the top of the fuel column where restructuring occurred in the breached element (J507) due to bond sodium loss.

Visual examination of the U-8Pu-10Zr fuel from XY-27, element J-486, revealed a large globule of sodium located on the face of the thinned area. Weighing of the element showed a decrease of 2.60 grams (sodium bond and fission gas accumulation). Element J-486 achieved a peak burnup of 6.6 at.%. Plenum gas analysis showed a volume of 2.54 cc and pressure of 57 psia (room temperature). Gamma scans indicated that the sodium bond was expelled through the breach. As in the case of the two previous breach elements (XY-21A and XY-24), metallographic exams revealed a small pin-hole type crack in the face of the thinned area and some restructuring at the top of the fuel column due to bond sodium loss.

Fig. 3. XY-24: Fuel Clad Interaction and Restructuring Comparisons



Element J507 (Breach)

Element J516 (No Breach)

The second U-8Pu-10Zr fuel element, J-432, had breached as well, and irradiation examination results were very similar to those of its sister element J-486 (Fig. 4). Weight loss was 2.45 grams. A plenum volume of 2.47 cc, at a pressure of 145 psia (room temperature), indicating that a breach had occurred and all bond sodium and accumulated fission gases had been expelled. Element J-432 had achieved a peak burnup of 6.7 at.%. The breach consisted of a crack, and at the top of fuel column some restructuring was apparent, as in the case of J-486.

### DISCUSSION OF PHASE I

In the case of all the IFR metal fuel scoping tests, the breach results appeared to have a definite fission product release signature. Typically, upon onset of the breach, an increase in gas activity as well as a relatively small-sharp DN signal was observed. In the case of tagged elements, the tag was readily identifiable. Figure 5 shows the release process. In the case of XY-24 and XY-27, a pattern of small gas activity pulses were observed after the initial breach activity, evidently due to a continued accumulation of fission gas "burping" out of the crack at periodic intervals. None of the breaches provided any DN activity of a prolonged nature nor a very high DN signal. Calculation of time-to-rupture using fission gas pressure appears to be conservative, probably due to the presence of a relatively dense layer at the periphery of the fuel slug. This layer may distribute the stress at the deformation site, thereby delaying the instability that normally occurs in the final stages of creep rupture under biaxial gas pressure loading conditions.

Fig. 4. XY-27 Element J432 Breach

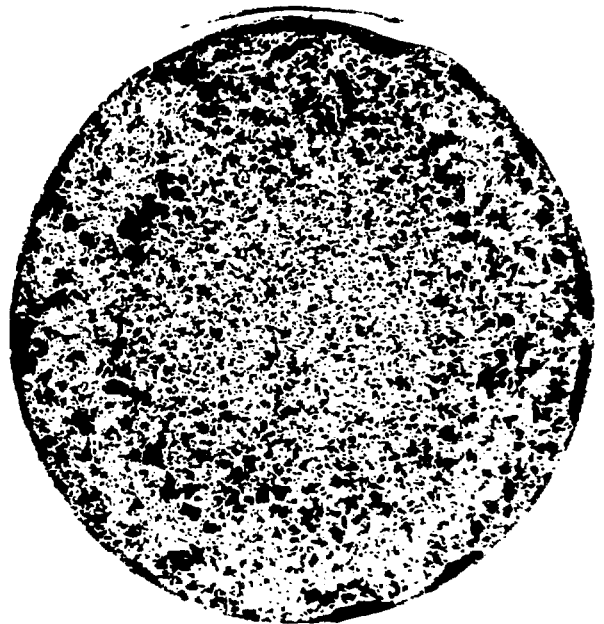
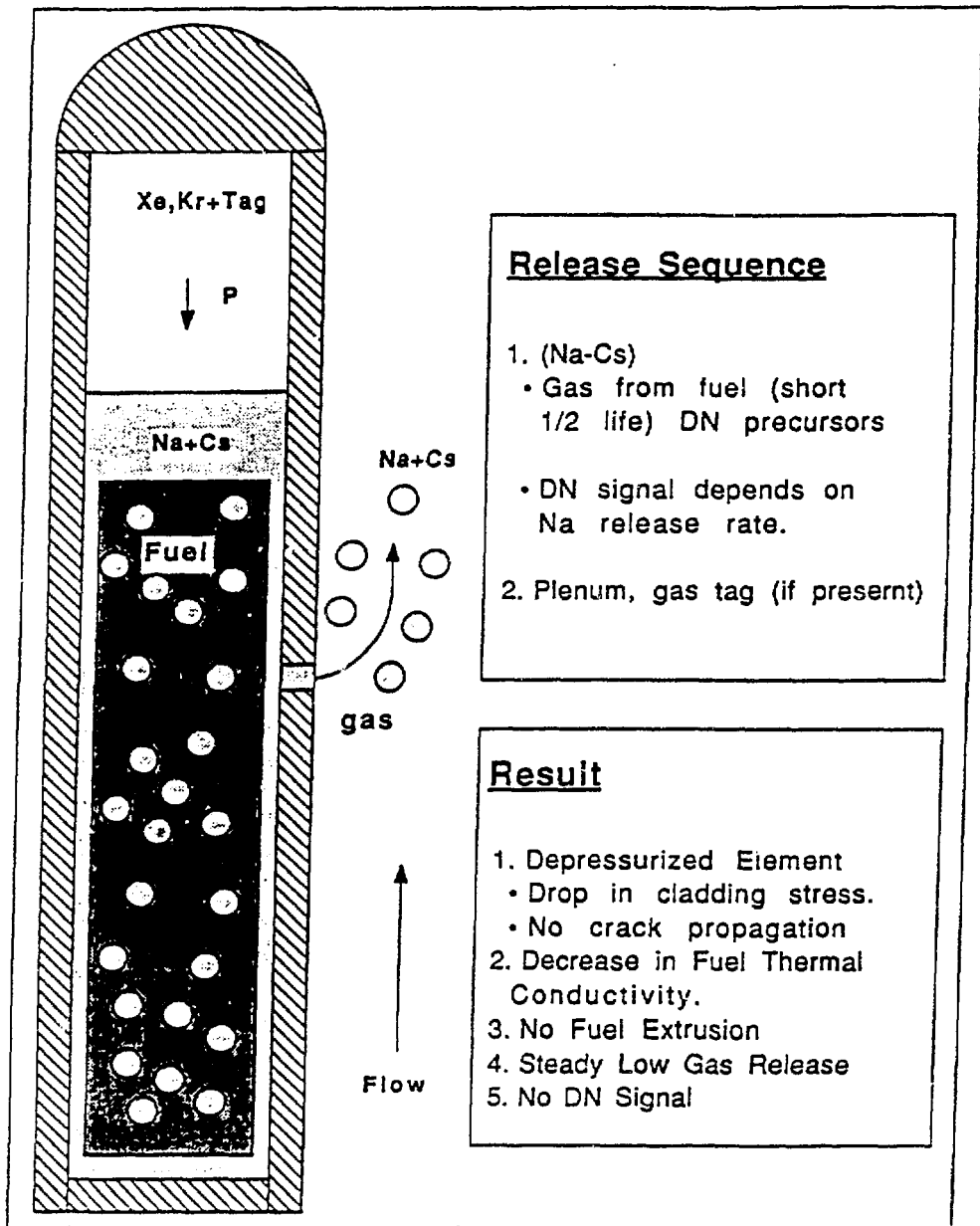


Fig. 5. Typical Release Sequence



PIE of breached elements revealed that no crack widening or fuel loss had occurred during prolonged RBCB irradiation. Only during the initial breach stage was there any evidence of significant release activity. After sodium bond and fission gas expulsion, release activity (with the exception of small "burps" of gas) ceased. Based on the results of the scoping tests, a more aggressive series of IFR prototypical fuel/element RBCB experiments were planned and initiated.

## PHASE II

This second phase of the program utilized previously irradiated IFR fuel pins (> 10 at.% burnup) to study the effects of breached operation on prototypical fuel. Table I provides a description of the three experimental subassemblies comprising phase II. As indicated, the data provided by the experiments are limited as one of the three experiments has undergone postirradiation exams as of yet.

Also different from the scoping tests was the position of the experiments within the core. The prototypical tests were run in open core positions. The test elements were defected in a manner similar to the test elements in the scoping experiments by thinning of the element clad at approximately core midplane.

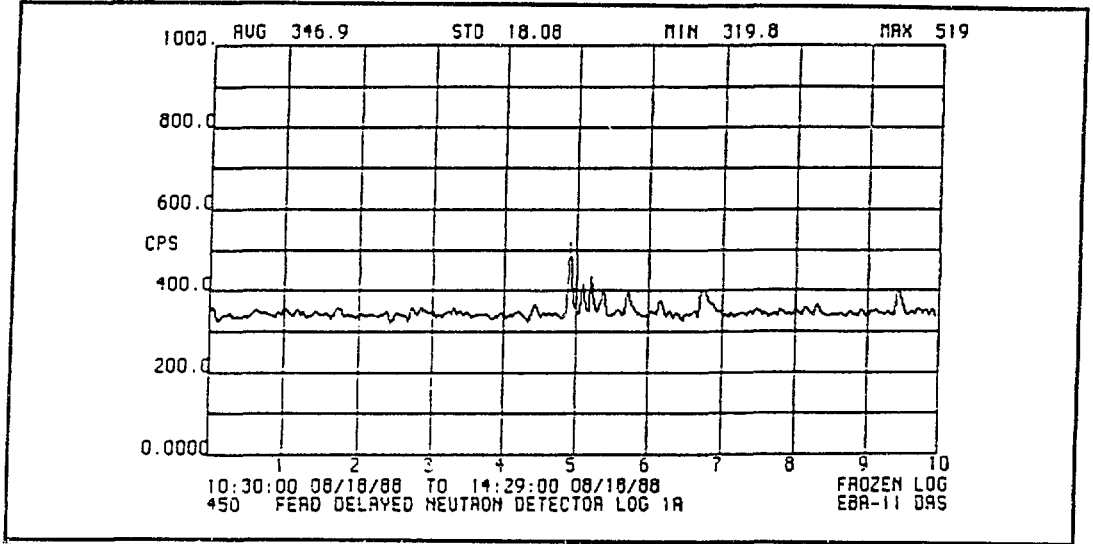
The materials tested in the prototypical IFR fuels were U-10Zr and U-19Pu-10Zr fuel; D9 and HT9 cladding. All three of the experiments were to be irradiated for approximately two reactor runs each.

The objectives to be achieved by the prototypical tests are:

- Observe general RBCB characteristics of IFR metal fuel in an open core position.
- Observe dynamics of a clad breach at above midplane elevation of an IFR metal fuel slug.
- Observe gas and DN signals to establish a characteristic "signature" for IFR prototypic elements at high burnup under RBCB conditions.
- Characterize fission product release and possible fuel loss from elements during extended RBCB operation.
- Characteristic changes in thermal conditions of fuel due to sodium expulsion upon breach.
- Observe changes in fuel cladding/chemical interaction after breach.

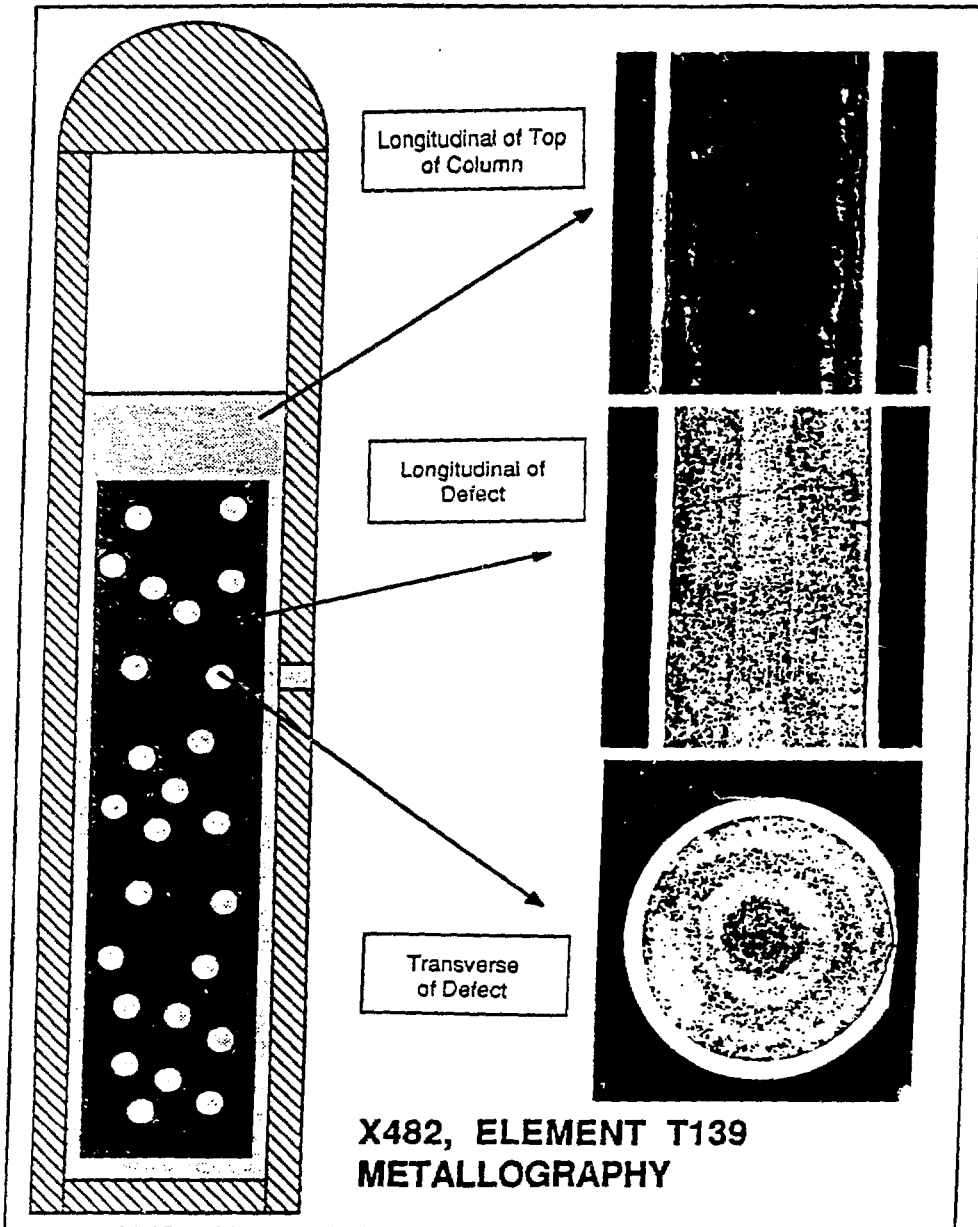
The prototypical tests performed thus far have demonstrated the same characteristic pattern as the scoping tests (see Table I). In experiments X482 and X482A, short duration DN signals of  $\Delta DN \sim 150$  cps were observed (Fig. 6). After the sodium bond, liquid fission products, DN precursors, and accumulated fission gas expulsion, activity ceased, with exception of periodic small "burps" of gas. Also, no further crack widening after initial breach takes place and negligible fuel loss is found in the prototypical tests (Fig. 7).

Fig. 6. X482 DN Signal During Breach



**X482**

Fig. 7. X482 Metallographic Exams



It is of interest to note that during the irradiation of one of the initial lead IFR tests a natural breach occurred in a D9 clad element. The test, X420, was removed from the reactor at ~16.4 at.% burnup for Post Irradiation Exams (PIE). Element T084 was identified as the breached element.

A good estimate of the breach burnup can be made since tag gas signals and delayed neutron signals were coincident. The failure site is a hairline crack in the fuel region of this U-19Pu-10Zr element, ~9 in. from the bottom of the fuel column ( $X/L_0=0.67$ ). Expulsion of bond sodium and fission products led to a delayed neutron signal as a burst of ~20 minute duration, approximately four (4) times background.

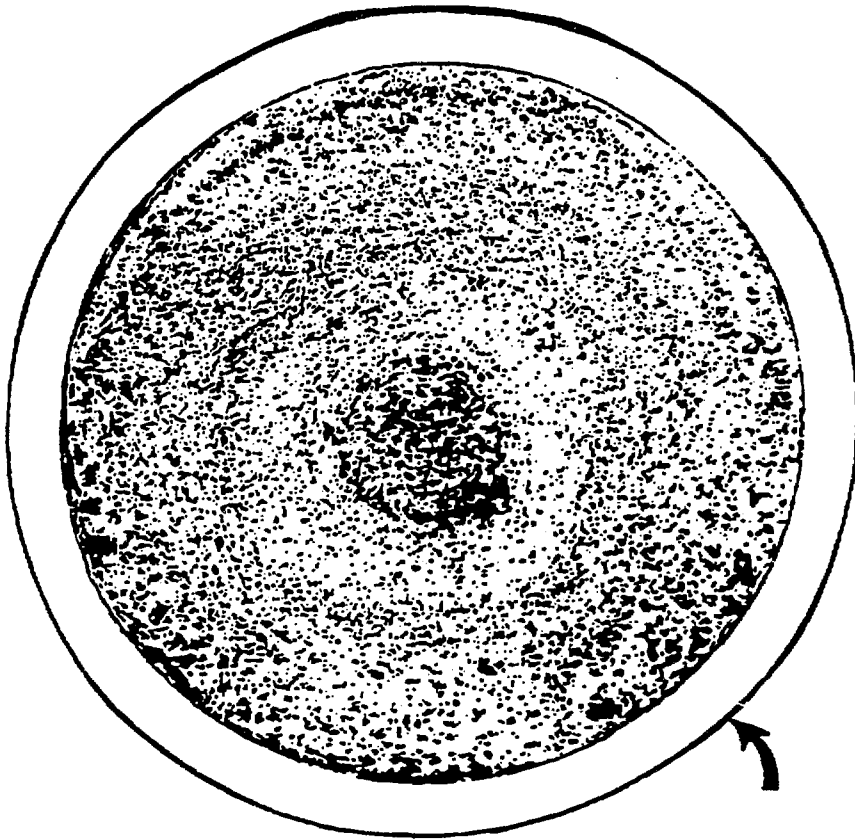
At the cladding outer surface, the crack is ~0.20 in. long by ~0.0002 in. wide and runs parallel to the element long axis (perpendicular to the cladding hoop stress). The main crack is intergranular with a few smaller cracks 2 to 3 grain diameters long clustered nearby. A shallow longitudinal "groove" could be seen on top of and adjacent to the main crack, possibly caused by abrasion with an adjacent element in this tight bundle of highly strained test elements (2/3 of the elements in the bundle has ~4% strain at this location). The crack was opposite T084's own wrapper wire at an azimuthal position where element/element interaction is maximum and tends to flatten the normal cladding circular cross-section. Laser profilometry confirmed the cladding ovality at this elevation.

The crack occurred in an area of intense fuel/cladding solid state interaction which was revealed by an oxalic acid etch. The maximum depth of interaction was ~0.15 mm (~0.006 in.) and was centered on an

azimuthal arc of increased interaction of  $\sim 30^\circ$ . Their interaction involved an interdiffusion of Ni and Fe from the cladding with the one authorized series of fission products. The fuel itself appeared to be unaffected by the breach as can be seen in the as-polished section in Fig. 8. The annular zones of redistribution were concentric and resembled sibling fuel at like burnup. It is clear that fuel loss in this type of breach is not to be expected. Microhardness values in the interaction layer showed the usual degree of hardening ( $\sim 750$  DPH higher than the unaffected cladding). However, the D9 base metal along the crack path had lower hardness values than samples  $90^\circ$  and  $180^\circ$  away (typically 50 DPH less). It would appear that based on the observations of accelerated fuel/cladding chemical interaction and the cladding softening, nominal cladding temperatures were exceeded for an indeterminate amount of time in reactor. At this high burnup, cladding dilation, and thermal bow possibly promoted local regions of distorted geometry and coolant flow. Stress rupture of the cladding would thus be promoted in areas of high cladding wastage and lowered creep strength.

EBR-II operated without consequence of this fuel column breach to the scheduled end of the run for an additional 34 days ( $\sim 0.6$  at.% burnup). Figure 9 illustrates the similarity between the breach DN signals of the natural breach that occurred in Test X420 and that of the artificially induced breach of one of the RBCB Tests, X482.

Fig. 8. Transverse section through the fuel column breach site. The arrow indicates location of the crack which is not visible at this magnification.



Although many exams have not been performed on the prototypical tests, the data obtained thus far, taken with the scoping test results, indicate an overall very benign RBCB behavior of IFR metallic fuel.

Two future tests are planned to demonstrate crack propagation of a clad breach and what would happen if an element of fresh fuel were to have a lower end weld defect.

Because of the restructuring observed at the top of the fuel column after breach, a question arose as to what would occur if a lower end breach occurred prior to the fuel swelling out to the clad at ~1 at.% burnup. An experiment is being proposed to demonstrate this event which could possibly arise during fabrication (i.e., lower end weld defect). It would be expected that the fission sodium would be expelled during fission gas buildup leaving a void between the fuel column and clad. The resultant gas gap would therefore lower the thermal conductivity, causing overheating and fuel restructuring.

As indicated in previous experiments, much data remains to be analyzed and questions relating to the breach performance of metal fuels still need to be answered. But results to date indicate that metallic fuel behavior is relatively benign and predictable allowing prolonged and safe operation in a breached condition.

Fig. 9 compares the DN signals from the artificially induced breach of the IFR RBCB experiment X482 with that of the naturally occurring breach in the lead IFR subassembly X420. Note the similarities in the initial short duration "spikes" followed by the signal return to background.